# Bose-Einstein Condensate in a Honeycomb Optical Lattice: Fingerprint of Superfluidity at the Dirac Point

Zhu Chen (陈竹)[1] and Biao Wu (吴飙)[2]

[1]*Institute of Physics, Chinese Academy of Sciences, 100190, Beijing, China*
[2]*International Center for Quantum Materials, Peking University, 100871, Beijing, China*

Mean-field Bloch bands of a Bose-Einstein condensate in a honeycomb optical lattice are computed. We find that the topological structure of the Bloch bands at the Dirac point is changed completely by atomic interaction of arbitrary small strength: the Dirac point is extended into a closed curve and an intersecting tube structure arises around the original Dirac point. These tubed Bloch bands are caused by the superfluidity of the system. Furthermore, they imply the inadequacy of the tight-binding model to describe an interacting Boson system around the Dirac point and the breakdown of adiabaticity by interaction of arbitrary small strength.

PACS numbers: 67.85.Hj, 03.75.Kk, 37.10.Jk

Inspired by the exciting physics in graphene [1–4], there have been increasing efforts to study ultracold atoms in a honeycomb optical lattice [5–11]. The primary reason is that these ultracold atom systems offer more controlling flexibilities over graphene [12,13]. For example, with this hexagonal ultracold atom system, one can readily change the lattice strength, tune the atomic scattering strength with Feshbach resonance, and load either bosons or fermions or even a mixture of bosons and fermions in the lattice. There have already been efforts to study conical diffraction [6–8] and observe quantum phases with ultracold bosons in a honeycomb lattice [9]. This controlling flexibility will not only offer deeper insight into the graphene properties but also open up windows for physics beyond graphene.

In this Letter we provide an insight into the interplay between superfluidity and Dirac dynamics by studying a Bose-Einstein condensate (BEC) in a honeycomb optical lattice. To showcase the interplay, we compute the lowest Bloch bands for this BEC system. We find that the topology of the Bloch bands around the Dirac point is completely altered by arbitrary small atomic interaction: an intersecting tube structure appears and the Dirac point is turned into a closed curve. We show that the topological change can be viewed as a permanent fingerprint left in the Bloch bands by superfluidity. As the interaction does not change the Dirac point structure in the tight-binding model, this topological change suggests that the tight-binding model is insufficient to describe the bosonic dynamics in a honeycomb lattice no matter how deep the lattice is. At the same time, these tubed bands imply the breakdown of adiabaticity by arbitrary small atomic interaction. A feasible experimental scheme is suggested to observe this phenomenon.

The honeycomb optical lattice can be experimentally realized by three interfering traveling laser beams [14,15], and is described mathematically by

$$V(\mathbf{r}) = V_0[\cos(\mathbf{b}_1 \cdot \mathbf{r}) + \cos(\mathbf{b}_2 \cdot \mathbf{r}) + \cos((\mathbf{b}_1 + \mathbf{b}_2) \cdot \mathbf{r})], \quad (1)$$

where the reciprocal unit vectors $\mathbf{b}_1 = 2\pi(\sqrt{3}, 1)/(3a)$ and $\mathbf{b}_2 = 2\pi(-\sqrt{3}, 1)/(3a)$ with $a = 2\lambda_L/3\sqrt{3}$. $\lambda_L$ is the wavelength of the laser beams. We are interested in the superfluid regime, where the BEC system can be well described by the Gross-Pitaevskii (GP) equation

$$i\hbar \frac{\partial \psi}{\partial t} = -\frac{\hbar^2}{2m}\nabla^2 \psi + V(\mathbf{r})\psi + \frac{4\pi\hbar^2 a_s}{m}|\psi|^2\psi, \quad (2)$$

with $m$ the mass of particle and $a_s$ the scattering length. For numerical computation, the above equation is made dimensionless by normalizing the wave function and choosing $6E_R$ as energy unit with $E_R = \hbar^2 k_L^2/2m$, $\hbar/6E_R$ as the time unit, and $\sqrt{3}a/2\pi$ as the length unit. The scaled nonlinearity and potential strength are denoted as $c$ and $v$, respectively.

We compute the Bloch wave solutions of the GP equation, which are of the form $\psi_{\mathbf{k}}(\mathbf{r}) = \sum_{m,n} c_{mn} e^{i(\mathbf{k}+\mathbf{G}_{mn})\cdot\mathbf{r}}$ with $\mathbf{G}_{mn} = m\mathbf{b}_1 + n\mathbf{b}_2$, and the corresponding nonlinear Bloch bands. The bands along the high-symmetry points are plotted in Fig. 2. Compared to the linear bands in Fig. 2 (a), we see that the nonlinear bands in (b) have a similar overall structure. However, the part around the Dirac point appears to be modified by nonlinearity. When it is enlarged, we find in (c) that the two linear bands have split into four bands. As a result, two more additional crossing points $D_1$ and $D_2$ appear while the Dirac crossing $D$ is shifted away from point $\mathbf{K}$. This feature is also clear in (d), where the Bloch band along the direction 30° off the $\mathbf{K}$-$\mathbf{M}$ axis is plotted. We have also plotted the nonlinear Bloch band near point $\mathbf{M}$ in Fig. 4(b) where we see a loop structure, very similar to the BEC Bloch bands in one dimensional optical lattice [16–18].

The full BEC Bloch bands near point $\mathbf{K}$ are plotted in Fig. 3(a). The complicated Bloch bands consist of three
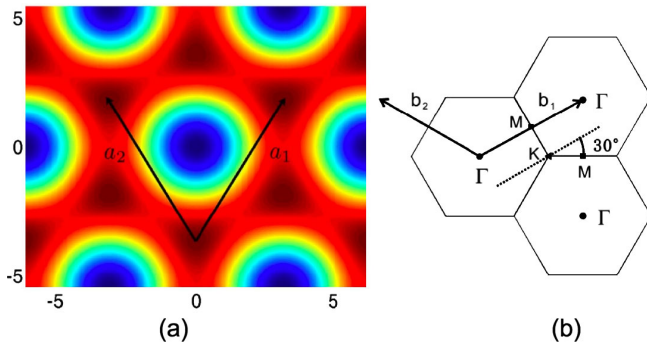
FIG. 1 (color online). (a) Contour map of the hexagonal potential in Eq. (1). The potential well is represented in red and the barrier in blue. The unit vectors are marked as $\mathbf{a}_1$ and $\mathbf{a}_2$. (b) Unit cell in the reciprocal space with unit vectors $\mathbf{b}_1$, $\mathbf{b}_2$ and the high-symmetry points $\mathbf{\Gamma}$, $\mathbf{M}$, and $\mathbf{K}$.

"tubes," which intersect at point $\mathbf{K}$ [see Fig. 3(b)] and are sandwiched by two Dirac cones. One of the tubes is shown in Fig. 3(c): it lies along the $\mathbf{M}$-$\mathbf{K}$ direction and it has a wedged cross section with an area increasing monotonically from $\mathbf{M}$ to $\mathbf{K}$. Figure 3(d) shows how two tubes intersect. The two white dots mark the top and bottom tips of this intersection and correspond to $D_1$ and $D_2$ points in Figs. 2(c) and 2(d). The green dots indicate part of a closed curve, which results from the intersection of the three tubes; the shifted Dirac point $D$ in Figs. 2(c) and 2(d) is one of the points on this closed curve. This shows that the Dirac point is turned into a closed curve by the interaction. The three tubes become smaller as the interaction strength $c$ gets weaker. In particular, as $c$ decreases, the tube will disappear first at point $\mathbf{M}$ and start shrinking toward point $\mathbf{K}$. However, surprisingly, the tubes never disappear com-

pletely at $\mathbf{K}$ as long as $c$ is not zero. This indicates that the tubed Bloch bands appear for arbitrary small interaction. Note that the tips of the Dirac cones in Fig. 3(a) have only triangular symmetry, and do not have the cylindrical symmetry as in the linear case.

The tubed structure can be viewed as a fingerprint left in the Bloch bands by the superfluidity of the BEC systems. Assume that we have a mass flow of boson particles, which is represented by plane wave $e^{i\mathbf{k}\cdot\mathbf{x}}$ with $\mathbf{k}$ at the Brillouin zone (BZ) edge point $\mathbf{M}$. We now slowly turn on an optical lattice of small lattice strength. For free bosons, the flow is stopped by the Brag scattering, the plane wave assumes the form of $\sin(\mathbf{k} \cdot \mathbf{x})$. In the energy band, this is reflected by that the crossing of two plane wave energy bands at $\mathbf{M}$ is replaced by a gap as seen in Fig. 4(a). In the nonlinear case, the situation can be very different: when the interaction is strong so that the superfluid critical velocity is larger than $|\mathbf{k}|$, the small optical lattice, which can be regarded as perturbation, should not stop the superflow. This implies that the wave function describing the flow should still resemble the plane wave $e^{i\mathbf{k}\cdot\mathbf{x}}$, and at the same time, the crossing of plane wave energy bands should remain unchanged. This is confirmed by our numerical calculation shown in Fig. 4(b). When this superfluidity argument is applied to other points along the BZ edge, we should have a tubed structure seen in Fig. 3. In other words, we can view the tubed structure as the fingerprint left in the BEC Bloch bands by superfluidity. For this hexagonal BEC system, this fingerprint stays as long as $c$ is not zero.

We emphasize that the appearance of the tubed structure in the BEC Bloch bands for arbitrary small $c$ is a unique feature for a honeycomb lattice: In one dimensional lattice [16–22] and two dimensional square lattice [23,24], the
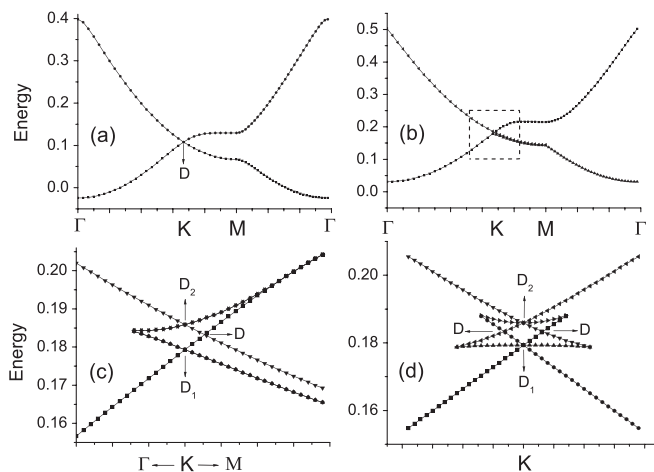


FIG. 2. Bloch bands along the high-symmetry points. (a) The linear case. $c = 0$, $v = 0.1$. $D$ marks the Dirac point at point $\mathbf{K}$. (b) The nonlinear case. $c = 0.1$, $v = 0.1$. (c) The enlarged rectangle part in (b). There appear two additional crossing points $D_1$ and $D_2$ while the linear Dirac point $D$ is shifted away from $\mathbf{K}$. (d) The band structure along the direction represented by the dashed line in Fig. 1(b).
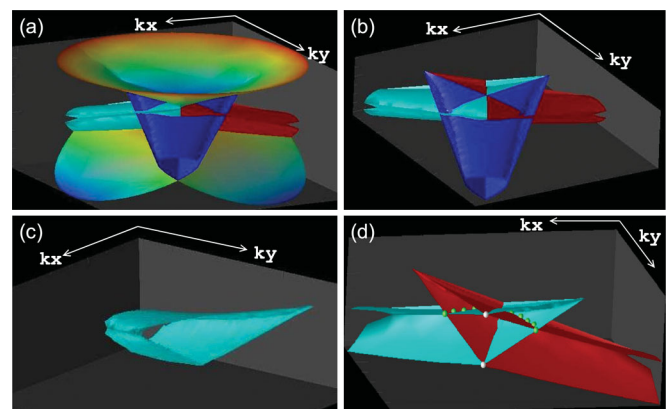


FIG. 3 (color). (a) The lowest nonlinear Bloch bands around point $\mathbf{K}$. They consist of three intersecting "tubes," which are sandwiched by two Dirac cones. (b) Three intersecting "tubes," which are aligned along the three $\mathbf{K}$-$\mathbf{M}$ axes; (c) one of three "tubes," whose cross-section area increases monotonically from $\mathbf{M}$ to $\mathbf{K}$; (d) the cross section of two intersecting "tubes." The white dots are $D_1$ and $D_2$ points in Fig. 2(c) while the green dots indicate a closed curve where the $D$ point in Fig. 2(c) belongs. $v = 0.1$, $c = 0.1$.
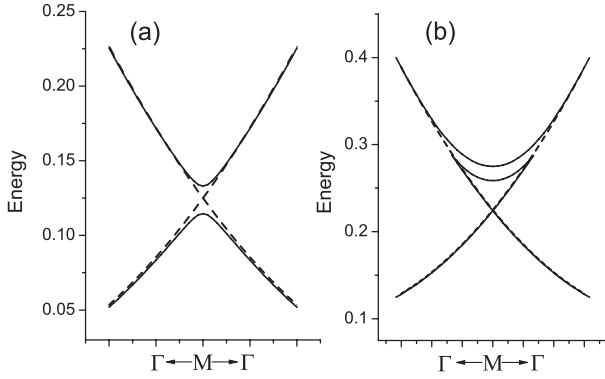
FIG. 4.    The lowest Bloch bands for a honeycomb lattice at the
**Γ**-**M**-**Γ** branch. (a) Free boson; (b) BEC. The solid curves are
Bloch bands while the dashed curves are the energy of the plane
waves.

looped or tubed nonlinear structure in the Bloch bands
appears only when $c$ is bigger than a threshold value.
This unique feature has a profound implication when the
tight-binding limit is considered. As is well known, when
the lattice is deep, it is believed that the system should be
well described by a tight-binding model [25]. However, as
shown below, the tight-binding model is not an adequate
approximation for a BEC in a honeycomb lattice no matter
how deep the lattice is.

Following the usual procedure [10,25], we write the
bosonic field as a sum over the two sublattices $\psi = \sum_{\vec{a}} \psi_{\vec{a}} u(\vec{r} - \vec{a}) + \sum_{\vec{b}} \psi_{\vec{b}} u(\vec{r} - \vec{b})$, where $u(\vec{r})$ is the
Wannier function and $\vec{a}$ and $\vec{b}$ are lattice vectors in the
two sublattices, respectively. Then the tight-binding
Hamiltonian for our BEC system is

$$H = -\sum_{\langle \vec{a},\vec{b}\rangle} J_{\vec{\delta}}(\psi_{\vec{a}}^* \psi_{\vec{b}} + \text{H.c.}) + \frac{U}{2}\Big[\sum_{\vec{a}}|\psi_{\vec{a}}|^4 + \sum_{\vec{b}}|\psi_{\vec{b}}|^4\Big],$$

(3)

where $J_{\vec{\delta}}$ is the hopping constant with $\vec{\delta}$ indicating three
different neighbors and $U$ is the on-site interaction propor-
tional to $c$. The ground state energy of this Hamiltonian is
$E = \pm|\Sigma_1| + U/2$, where $\Sigma_1 = -\sum_{\vec{\delta}} J_{\vec{\delta}} e^{i\mathbf{k}\cdot\vec{\delta}}$. This shows
that the interaction has only a trivial effect on the band
structure, lifting the Dirac bands by a constant $U/2$. This is
very different from the GP equation result, where arbitrary
small interaction can destroy the Dirac bands. This surpris-
ing difference implies that the tight-binding model cannot

describe well the BEC system in a honeycomb lattice no
matter how deep the lattice is.

After careful analysis, we find that the inadequacy of the
tight-binding model may be caused by the inappropriate
choice of Wannier functions. Let us consider the linear
case where $J_{\vec{\delta}1} = J_{\vec{\delta}2} = J$ and $J_{\vec{\delta}3} > J$ [26]. Its Bloch
bands around point **K** are plotted as solid lines in Fig. 5,
where one immediately notices that the Dirac point is
shifted as we also see in Fig. 2. To have a different $J_{\vec{\delta}3}$,
one needs a set of Wannier functions which have no three-
fold rotational symmetry. This seems to suggest that the
choice of Wannier functions, which are used to obtain the
tight-binding model, depends on the state of the system.
Conventionally, the choice of Wannier functions is inde-
pendent of the state of the system. If this were indeed the
case, one would expect to have for another state a set
of Wannier functions, which yield $J_{\vec{\delta}1} = J_{\vec{\delta}3} = J$ and
$J_{\vec{\delta}2} > J$. The Bloch bands for this case are plotted as
dashed lines in Fig. 5, where the band splitting at point
**K** is another feature seen in Fig. 2. To fully establish this
view, more computation needs to be done and will be
carried out in the future. One possible way of doing the
computation is to use the method proposed in Ref. [27].

Interestingly, the tubed structure shown in Fig. 3 has
another important physical implication, the breakdown of
adiabaticity by nonlinearity. In the linear case, the state of
the system can adiabatically follow the lower left band to
the upper right band by passing through the Dirac point. In
the nonlinear case, this adiabatic following is broken. This
can be seen clearly in Fig. 2(d): the system can follow
adiabatically passing point $D$ till the tip of the band, where
no more band to follow and the adiabaticity is broken. This
type of breakdown of adiabaticity is also implied in the
loop structure in one dimensional optical lattice. Such an
interesting effect has not only been generalized to general
nonlinear quantum systems [28] but also been observed
experimentally with ultracold atoms [29]. The uniqueness
of the hexagonal system is that the breakdown of adiaba-
ticity occurs for arbitrary small interaction whereas it
happens only when the nonlinearity is bigger than a thresh-
old value in the 1D system or other previously studied
systems.

Note that this interesting phenomenon is not limited to
the system of BEC in a honeycomb lattice. It can be seen
clearly when we approximate this BEC system at point **K**
with a three-mode model. The three-mode model is

$$i\frac{\partial}{\partial t}\begin{pmatrix}\phi_1 \\ \phi_2 \\ \phi_3\end{pmatrix} = \begin{pmatrix} -|\phi_1|^2 c - \frac{\delta k_x}{4} - \frac{\sqrt{3}\delta k_y}{4} & v/2 & v/2 \\ v/2 & -|\phi_2|^2 c + \frac{\delta k_x}{2} & v/2 \\ v/2 & v/2 & -|\phi_3|^2 c - \frac{\delta k_x}{4} + \frac{\sqrt{3}\delta k_y}{4} \end{pmatrix}\begin{pmatrix}\phi_1 \\ \phi_2 \\ \phi_3\end{pmatrix},$$

(4)

where $\delta k_x$ and $\delta k_y$ denote how much the Bloch wave
number **k** deviates away from **K**. This three-mode model

can also describe a BEC in a triple-well potential, where
the three wells are arranged in a triangular geometry

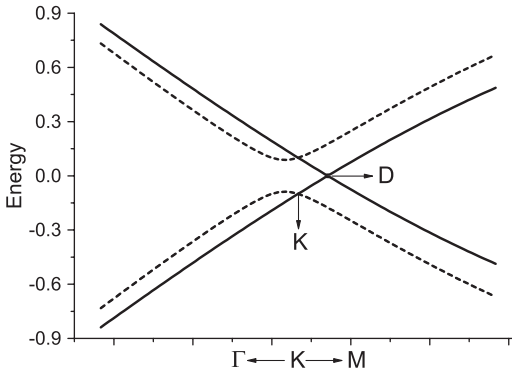FIG. 5. The linear Bloch bands of the tight-binding model along the **Γ**-**K**-**M** branch. Solid lines are for $J_{\tilde{\delta}_1} = J_{\tilde{\delta}_2} = J$ and $J_{\tilde{\delta}_3} = 1.1J$ and dashed lines are for $J_{\tilde{\delta}_1} = J_{\tilde{\delta}_3} = J$ and $J_{\tilde{\delta}_2} = 1.1J$. The resemblance to Fig. 2(c) is clear. The vertical axis is the energy in the unit of $J$.

with the depth of each well adjustable [30,31]. It should also be realizable in experiment with waveguide systems [32–34] and other nonlinear optical systems. This shows that this breakdown of adiabaticity by arbitrary small interaction is general and can happen in a wide range of systems.

Inspired by the experiment in [29], we here propose a scheme to realize the above mentioned triple-well configuration. The procedure is as follows. At first, a triangular lattice is formed by three lasers. The triangular potential can be described by $V_{\text{tri}} = V_0[\cos(x + \frac{y}{\sqrt{3}}) + \cos(-x + \frac{y}{\sqrt{3}}) + \cos(\frac{2y}{\sqrt{3}})]$ with $V_0 < 0$. The second step is to form the triple-well systems by adding a rectangular lattice $V_{\text{rec}}(\theta, \varphi) = V_1[\cos(x/2 + \theta) + \cos(y/\sqrt{3} + \varphi)]$ ($V_1 > 0$). As $\theta$, $\varphi$ changes, the second optical lattice can not only break the triangular lattice into a series of independent triple-well systems but also change the depth of each well. One should be able to demonstrate the breakdown of adiabaticity by arbitrary small interaction with this triple-well system, similar to the experiment done in Ref. [29].

In sum, we have computed the BEC Bloch bands in a honeycomb optical lattice. Our results show that a tube-intersecting structure can emerge between the up and down Dirac cones for arbitrary small interaction. This structure has two interesting physical implications: (1) the tight-binding model cannot describe adequately the BEC in a honeycomb lattice even when the lattice is very deep; (2) the adiabaticity can be broken down by arbitrary small interaction in certain systems. For the latter, we have proposed an experimental scheme to observe it.

[1] K. S. Novoselov *et al.*, Nature (London) **438**, 197 (2005).
[2] Yuanbo Zhang, Yan-Wen Tan, Horst L. Stormer, and Philip Kim, Nature (London) **438**, 201 (2005).
[3] C. Wu, D. Bergman, L. Balents, and S. DasSarma, Phys. Rev. Lett. **99**, 070401 (2007).
[4] Wang Yao, Shengyuan A. Yang, and Qian Niu, Phys. Rev. Lett. **102**, 096801 (2009).
[5] S. L. Zhu, Baigeng Wang, and L.-M. Duan, Phys. Rev. Lett. **98**, 260402 (2007).
[6] M. J. Ablowitz, S. D. Nixon, and Y. Zhu, Phys. Rev. A **79**, 053830 (2009).
[7] O. Bahat-Treidel, O. Peleg, M. Segev, and H. Buljan, Phys. Rev. A **82**, 013830 (2010).
[8] O. Peleg, G. Bartal, B. Freedman, O. Manela, M. Segev, and D. N. Christodoulides, Phys. Rev. Lett. **98**, 103901 (2007).
[9] Parvis Soltan-Panahi *et al.*, Nature Phys. **7**, 434 (2011).
[10] L. H. Haddad and L. D. Carr, Europhys. Lett. **94**, 56002 (2011).
[11] L. H. Haddad and L. D. Carr, Physica (Amsterdam) **238D**, 1413 (2009).
[12] O. Morsch and M. Oberthaler, Rev. Mod. Phys. **78**, 179 (2006).
[13] V. Yukalov, Laser Phys. **19**, 1 (2009).
[14] G. Grynberg, B. Lounis, P. Verkerk, J. Y. Courtois, and C. Salomon, Phys. Rev. Lett. **70**, 2249 (1993).
[15] B. Wunsch, F. Guinea, and F. Sols, New J. Phys. **10**, 103027 (2008).
[16] B. Wu and Q. Niu, New J. Phys. **5**, 104 (2003).
[17] B. Wu and Q. Niu, Phys. Rev. A **61**, 023402 (2000).
[18] M. Machholm, C. J. Pethick, and H. Smith, Phys. Rev. A **67**, 053613 (2003).
[19] B. T. Seaman, L. D. Carr, and M. J. Holland, Phys. Rev. A **71**, 033622 (2005).
[20] B. T. Seaman, L. D. Carr, and M. J. Holland, Phys. Rev. A **72**, 033602 (2005).
[21] E. J. Mueller, Phys. Rev. A **66**, 063603 (2002).
[22] B. P. Venkatesh, J. Larson, and D. H. J. O'Dell, Phys. Rev. A **83**, 063606 (2011).
[23] Z. Chen, Z. Liang, and B. Wu (unpublished).
[24] C.-S. Chien, S.-L. Chang, and B. Wu, Comput. Phys. Commun. **181**, 1727 (2010).
[25] A. Smerzi, A. Trombettoni, P. G. Kevrekidis, and A. R. Bishop, Phys. Rev. Lett. **89**, 170402 (2002).
[26] K. L. Lee, B. Grémaud, R. Han, B.-G. Englert, and C. Miniatura, Phys. Rev. A **80**, 043411 (2009).
[27] B. Wu and J. Shi, arXiv:0907.2046v1.
[28] J. Liu, B. Wu, and Q. Niu, Phys. Rev. Lett. **90**, 170404 (2003).
[29] Y.-A. Chen, S. D. Huber, S. Trotzky, I. Bloch, and E. Altman, Nature Phys. **7**, 61 (2011).
[30] R. Franzosi and V. Penna, Phys. Rev. E **67**, 046227 (2003).
[31] X. Jiang, L.-B. Fu, W.-S. Duan, and J. Liu (to be published).
[32] X. Luo, Q. Xie, and B. Wu, Phys. Rev. A **76**, 051802(R) (2007).
[33] A. Szameit *et al.*, Opt. Lett. **34**, 2700 (2009).
[34] A. S. Desyatnikov *et al.*, Opt. Lett. **32**, 325 (2007).